

Cold QCD at finite isospin density: confronting effective models with recent lattice data

Sidney S. Avancini,¹ Aritra Bandyopadhyay,² Dyana C. Duarte,³ and Ricardo L. S. Farias²

¹*Departamento de Física, Universidade Federal de Santa Catarina, 88040-900 Florianópolis, Santa Catarina, Brazil*

²*Departamento de Física, Universidade Federal de Santa Maria, Santa Maria, RS 97105-900, Brazil*

³*Departamento de Física, Instituto Tecnológico de Aeronáutica, 12228-900 São José dos Campos, SP, Brazil*

(Dated: September 3, 2022)

We compute the QCD equation of state for zero temperature and finite isospin density within the Nambu-Jona-Lasinio model in the mean field approximation, motivated by the recently obtained Lattice QCD results for a new class of compact stars: pion stars. We have considered both the commonly used Traditional cutoff Regularization Scheme and the Medium Separation Scheme, where in the latter purely vacuum contributions are separated in such a way that one is left with ultraviolet divergent momentum integrals depending only on vacuum quantities. We have also compared our results with the recent results from Lattice QCD and Chiral Perturbation Theory.

I. INTRODUCTION

Quantum chromodynamics (QCD) is the fundamental theory of strong interactions. QCD has a remarkably rich phase structure with multiple facets which has been vividly explored over the years. Recently, with the imminent arrival of relativistic Heavy-Ion-Collision (HIC) experiments in FAIR and NICA, physical systems at finite baryon densities such as neutron stars has become the ideal subject for scrutiny in the heavy ion community [1, 2]. However, systems with finite baryon densities are not easy to deal with theoretically, since in this region of QCD phase diagram, first-principle methods such as non-perturbative lattice calculations are not accessible due to the well known fermion “sign problem” [3, 4]. For a recent review about the progress of lattice QCD in dealing with sign problem, see Ref [5].

Aside the baryon chemical potential $\mu_B = 3(\mu_u + \mu_d)/2$ (for a 2-flavor system), QCD at finite density can also be characterized by the isospin chemical potential $\mu_I = (\mu_u - \mu_d)/2$. On the contrary to what happens at finite baryonic density, systems with finite isospin density does not suffer with the sign problem and hence are easily accessible to lattice QCD based calculations. Initial results of lattice QCD at finite temperature and isospin density appeared in early 2000’s [6, 7] and they were also investigated by other available techniques, such as chiral perturbation theory (χ PT) [8–17], Hard Thermal Loop perturbation theory (HTLpt) [18], Nambu-Jona-Lasinio (NJL) model [19–35] and its Polyakov loop extended version PNJL [36, 37], quark meson model (QMM) [38–41] and the results were largely in qualitative agreement. However, all of the early lattice QCD calculations have been done considering unphysical pion masses and/or an unphysical flavour content. Recently, this issue has been rectified by using an improved lattice action with staggered fermions at physical quark masses and the modified lattice QCD results for finite isospin density are presented in Refs [42–45].

Since the study of compact star interiors with high baryon densities are not accessible within lattice QCD

calculations, recently a different novel scenario has been proposed in Ref [46], where the pion condensates are considered to be the dominant constituent of the compact star core under the circumstance of vanishing neutron density. Study of this new type of compact stars, identified as pion stars, are easily accessible through first principle methods. Though pion stars can be described as a subset of boson stars [47–51], they are free from hypothetical beyond standard model contributions usually associated with boson stars, such as QCD axion. Indeed, it can be proved in the framework of a dense neutrino gas that a Bose-Einstein condensate of positively charged pions can be formed [52]. Further exploration of the pion stars’ Equation of State (EoS) revealed about its large mass and radius in comparison with neutron stars [46, 53]. Recently studies in the similar line have also been done within the chiral perturbation theory [54].

Though there are also possibilities of pion condensation in the early universe driven by high lepton asymmetry [52, 55, 56], in the current context we will consider the setting of compact stars with zero temperature. Further, the charged pion condensation requires accumulation of isospin charge at zero baryon density and zero strangeness. QCD with $\mu_I \neq 0$, $\mu_B = \mu_s = T = 0$ can be and is being realized well within lattice QCD and this new modified lattice result [46] in turn gives us the perfect platform for the consistency check of the effective models mimicking QCD, such as NJL model. As emphasized earlier, QCD with finite isospin chemical potential have already been explored through NJL model, albeit none in light of the new improved lattice results. Additionally the present study tries to rectify the regularization issues within NJL model to deal with the ultraviolet (UV) divergent momentum integrals. In the Traditional Regularization Scheme (TRS), commonly used in literature, the sharp UV cutoff Λ usually cuts important degrees of freedom near the Fermi surface leading to incorrect results, specially in scales of the order of Λ , e.g. $\mu_I \sim \Lambda$ [57, 58]. On the other hand, the Medium Separation Scheme (MSS), coined in Refs [59, 60], is based on a proper separation of medium effects from divergent

integrals, originally having explicit medium dependence. This results in the disposal of all divergent integrals into the pure vacuum part i.e. $\mu_I = 0$ in the current context, as it should be. This scheme has already been successfully applied in the context of color superconductivity [57] and for quark matter with a chiral imbalance [59]. For a proper characterization of compact pion stars with high values of μ_I ($\sim \Lambda$), as we will be dealing with in this work, the role of MSS becomes really important in this regard.

The paper is organized as follows. In section II we discuss the basic formalism of the two-flavor NJL model both within TRS and MSS. In section III we present our results obtained with the traditional regularization scheme and with the medium separation scheme, thermodynamic results are also presented and contrasted with other state of the art calculations. We conclude in section IV discussing the aftermath.

II. FORMALISM

In this section we revisit the well documented formalism for two-flavor NJL model with finite isospin chemical potential [23–35]. We start with the partition function for the two-flavor NJL model at finite baryonic and isospin chemical potential, given by

$$Z_{\text{NJL}}(T, \mu_B, \mu_I) = \int [d\bar{\psi}][d\psi] \times \exp \left[\int_0^\beta dt \int d^3x (\mathcal{L}_{\text{NJL}} + \bar{\psi} \hat{\mu} \gamma_0 \psi) \right], \quad (2.1)$$

where the quark chemical potential matrix in flavor space is

$$\hat{\mu} = \begin{pmatrix} \mu_u & 0 \\ 0 & \mu_d \end{pmatrix}, \quad (2.2)$$

and $\mu_{u,d}$ can be expressed in terms of the baryonic and the isospin chemical potential as

$$\begin{aligned} \mu_u &= \frac{\mu_B}{3} + \mu_I, \\ \mu_d &= \frac{\mu_B}{3} - \mu_I, \end{aligned}$$

such that $\mu_B/3 = (\mu_u + \mu_d)/2$ and $\mu_I = (\mu_u - \mu_d)/2$. \mathcal{L}_{NJL} appearing in Eq.(2.1) is the NJL Lagrangian considering scalar and pseudoscalar interactions, i.e.

$$\begin{aligned} \mathcal{L}_{\text{NJL}} &= \bar{\psi} (i\partial - m) \psi + G \left[(\bar{\psi}\psi)^2 + (\bar{\psi}i\gamma_5\vec{\tau}\psi)^2 \right], \\ &= \bar{\psi} (i\partial - m) \psi + G \left[(\bar{\psi}\psi)^2 + (\bar{\psi}i\gamma_5\tau_3\psi)^2 \right. \\ &\quad \left. + 2(\bar{\psi}i\gamma_5\tau_+\psi)(\bar{\psi}i\gamma_5\tau_-\psi) \right], \end{aligned} \quad (2.3)$$

where ψ and m represent the quark fields and their current mass respectively and G is the scalar coupling constant of the model. τ 's are the generator matrices for the

pseudoscalar interactions, which corresponds to the pion excitations π_1, π_2, π_3 or equivalently π_+, π_-, π_3 , with $\tau_\pm = (\tau_1 \pm \tau_2)/\sqrt{2}$.

For finite isospin chemical potential, the isospin symmetry group $SU(2)$ explicitly breaks down to a subgroup $U_I(1)$, third component of the isospin charge \mathbf{I}_3 being the generator [24]. So within the context of the mean field approximation, for nonzero μ_I one can consider the possibility of $\langle \bar{\psi}i\gamma_5\tau_3\psi \rangle = 0$ as an ansatz, which further breaks the $U_I(1)$ symmetry. Now we can introduce the chiral condensate $\sigma = -2G\langle \bar{\psi}\psi \rangle$ and pion condensates

$$\begin{aligned} \sqrt{2}\pi_+ &= -2\sqrt{2}G\langle \bar{\psi}i\gamma_5\tau_+\psi \rangle = \Delta e^{i\theta}, \\ \sqrt{2}\pi_- &= -2\sqrt{2}G\langle \bar{\psi}i\gamma_5\tau_-\psi \rangle = \Delta e^{-i\theta}, \end{aligned}$$

where the phase factor θ indicates the direction of the $U_I(1)$ symmetry breaking. Finally, for the present context of pion stars, we consider $\mu_B = 0$, such that $\mu_u = -\mu_d = \mu_I$. Putting all these together one can now obtain the thermodynamic potential within the mean field approximation as

$$\Omega_{\text{NJL}}(\sigma, \Delta) = \frac{\sigma^2 + \Delta^2}{4G} - 2N_c \int_\Lambda \frac{d^3k}{(2\pi)^3} \left[E_k^+ + E_k^- \right], \quad (2.4)$$

where $E_k^\pm = \sqrt{(E_k \pm \mu_I)^2 + \Delta^2}$ with $E_k = \sqrt{k^2 + M^2}$, $M = m + \sigma$ and the symbol \int_Λ indicates integrals that need to be regularized.

The physical values of the condensates vis-a-vis the ground state at finite isospin chemical potential is determined by minimizing $\Omega_{\text{NJL}}(\sigma, \Delta)$ with respect to the condensates σ and Δ , i.e. by solving the gap equations

$$\left. \frac{\partial \Omega_{\text{NJL}}}{\partial \sigma} \right|_{\sigma=\sigma_m} = \left. \frac{\partial \Omega_{\text{NJL}}}{\partial \Delta} \right|_{\Delta=\Delta_m} = 0. \quad (2.5)$$

From these equations we obtain

$$\sigma = 4GN_c M I_\sigma, \quad (2.6)$$

$$\Delta = 4GN_c \Delta I_\Delta, \quad (2.7)$$

with the definitions

$$I_\sigma = \sum_{s=\pm 1} \int_\Lambda \frac{d^3k}{(2\pi)^3} \frac{1}{E_k} \frac{E_k + s\mu_I}{\sqrt{(E_k + s\mu_I)^2 + \Delta^2}}, \quad (2.8)$$

$$I_\Delta = \sum_{s=\pm 1} \int_\Lambda \frac{d^3k}{(2\pi)^3} \frac{1}{\sqrt{(E_k + s\mu_I)^2 + \Delta^2}}. \quad (2.9)$$

In the following subsections we discuss with more details different ways of regularizing these integrals. The thermodynamic quantities, i.e. the pressure, the isospin density and the energy density of the system are then respectively given by

$$P_{\text{NJL}} = -\Omega_{\text{NJL}}(\sigma = \sigma_m; \Delta = \Delta_m), \quad (2.10)$$

$$\langle n_I \rangle_{\text{NJL}} = \frac{\partial P_{\text{NJL}}}{\partial \mu_I}, \quad (2.11)$$

$$\varepsilon_{\text{NJL}} = -P_{\text{NJL}} + \mu_I \langle n_I \rangle_{\text{NJL}}. \quad (2.12)$$

Finally, the EoS within the two-flavor NJL model is given by the relation between P_{NJL} and ε_{NJL} .

A. TRS

TRS is the most common and used regularization scheme in the literature, as might be seen in some good reviews of the NJL model [61]. In this case we just perform the integrations in (2.8) and (2.9) up to a cutoff Λ , that becomes a model parameter. Therefore, the gap equations becomes

$$\sigma = 4GN_c M \int_0^\Lambda \frac{k^2 dk}{2\pi^2} \sum_{j=\pm 1} \frac{E_k + j\mu_I}{E_k \sqrt{(E_k + j\mu_I)^2 + \Delta^2}} \quad (2.13)$$

$$\Delta = 4GN_c \Delta \int_0^\Lambda \frac{k^2 dk}{2\pi^2} \sum_{j=\pm 1} \frac{1}{\sqrt{(E_k + j\mu_I)^2 + \Delta^2}} \quad (2.14)$$

This same procedure is used in Ω_{NJL} , that becomes

$$\Omega_{\text{NJL}}^{\text{TRS}}(\sigma, \Delta) = \frac{\sigma^2 + \Delta^2}{4G} - 2N_c \int_0^\Lambda \frac{k^2 dk}{2\pi^2} [E_k^+ + E_k^-] \quad (2.15)$$

and also in the thermodynamic quantities. Specifically, the isospin density becomes

$$\langle n_I \rangle_{\text{NJL}}^{\text{TRS}} = -2N_c \int_0^\Lambda \frac{k^2 dk}{2\pi^2} \left[\frac{E_k - \mu_I}{E_k^-} - \frac{E_k + \mu_I}{E_k^+} \right]. \quad (2.16)$$

B. MSS

Since NJL is nonrenormalizable, any physical quantity will depend on the scale of the model Λ . However, it is very important to keep in mind that cutoff dependent medium terms due to a naive regularization of the integrals may lead to results completely different from the ones obtained with a more careful treatment of divergences. MSS provides a tool to disentangle medium dependencies from divergent contributions, so that only vacuum integrals remains to be regularized. This scheme has been applied to the NJL model and successfully shows qualitative agreement with lattice simulations and more elaborated theories, as might be seen in Refs. [57, 59, 60].

The implementation of MSS starts by rewriting, for example, I_Δ given in Eq. (2.9) as

$$I_\Delta = \frac{1}{\pi} \sum_{j=\pm 1} \int_{-\infty}^{+\infty} dx \int_\Lambda \frac{d^3 k}{(2\pi)^3} \frac{1}{x^2 + (E_k + j\mu_I)^2 + \Delta^2}. \quad (2.17)$$

Using the identity

$$\begin{aligned} & \frac{1}{x^2 + (E_k + j\mu_I)^2 + \Delta^2} \\ &= \frac{1}{x^2 + k^2 + M_0^2} \\ &+ \frac{M_0^2 - \Delta^2 - \mu_I^2 - M^2 - 2j\mu_I E_k}{(x^2 + k^2 + M_0^2)[x^2 + (E_k + j\mu_I)^2 + \Delta^2]} \end{aligned} \quad (2.18)$$

(where M_0 is the vacuum mass, when $\mu_I = \Delta = 0$) we obtain, after two iterations,

$$\begin{aligned} & \sum_{j=\pm 1} \frac{1}{x^2 + (E_k + j\mu_I)^2 + \Delta^2} \\ &= \frac{2}{x^2 + k^2 + M_0^2} + \frac{2\mathcal{M}}{(x^2 + k^2 + M_0^2)^2} \\ &+ \frac{2\mathcal{M}^2 + 8\mu_I^2 E_k^2}{(x^2 + k^2 + M_0^2)^3} \\ &+ \sum_{j=\pm 1} \frac{(\mathcal{M} - 2j\mu_I E_k)^3}{(x^2 + k^2 + M_0^2)^3 [x^2 + (E_k + j\mu_I)^2 + \Delta^2]} \end{aligned} \quad (2.19)$$

where we have defined $\mathcal{M} = M_0^2 - \Delta^2 - \mu_I^2 - M^2$. After some manipulations and performing the integration in x indicated in (2.17) we obtain

$$\begin{aligned} I_\Delta^{\text{MSS}} &= 2I_{\text{quad}} - (M^2 - M_0^2 + \Delta^2 - 2\mu_I^2)I_{\text{log}} \\ &+ \left[\frac{3(\mathcal{M}^2 + 4\mu_I^2 M^2)}{4} - 3\mu_I^2 M_0^2 \right] I_1 + 2I_2 \end{aligned} \quad (2.20)$$

with the definitions

$$I_{\text{quad}} = \int \frac{d^3 k}{(2\pi)^3} \frac{1}{\sqrt{k^2 + M_0^2}}, \quad (2.21)$$

$$I_{\text{log}} = \int \frac{d^3 k}{(2\pi)^3} \frac{1}{(k^2 + M_0^2)^{\frac{3}{2}}}, \quad (2.22)$$

$$I_1 = \int \frac{d^3 k}{(2\pi)^3} \frac{1}{(k^2 + M_0^2)^{\frac{5}{2}}}, \quad (2.23)$$

$$\begin{aligned} I_2 &= \frac{15}{32} \sum_{j=\pm 1} \int \frac{d^3 k}{(2\pi)^3} \int_0^1 dt (1-t)^2 \\ &\times \frac{(\mathcal{M} - 2j\mu_I E_k)^3}{[(2j\mu_I E_k - \mathcal{M})t + k^2 + M_0^2]^{\frac{7}{2}}}, \end{aligned} \quad (2.24)$$

where, in the last line of the equation above we have used the Feynman parametrization

$$\frac{1}{A_1^n A_2^m} = \frac{\Gamma(n+m)}{\Gamma(n)\Gamma(m)} \int_0^1 dt \frac{t^{n-1}(1-t)^{m-1}}{[A_1 t + A_2(1-t)]^{n+m}}. \quad (2.25)$$

Using similar steps one may write

$$\begin{aligned} I_\sigma^{\text{MSS}} &= 2I_{\text{quad}} - (M^2 - M_0^2 + \Delta^2)I_{\text{log}} + I_3 \\ &+ 3 \left[\frac{\mathcal{M}^2}{4} + \mu_I^2(M^2 - M_0^2 - \mathcal{M}) \right] I_1 + 2I_2, \end{aligned} \quad (2.26)$$

with

$$I_3 = \frac{15}{16} \sum_{j=\pm 1} \int \frac{d^3 k}{(2\pi)^3} \int_0^\infty \frac{t^2 dt}{\sqrt{1+t}} \times \frac{1}{E_k} \frac{j\mu_I (\mathcal{M} - 2j\mu_I E_k)^3}{[(k^2 + M_0^2)t + (E_k + j\mu_I)^2 + \Delta^2]^{\frac{7}{2}}} \quad (2.27)$$

Using MSS the expression for the normalized thermodynamic potential becomes

$$\Omega_{\text{NJL}}^{\text{MSS}}(\sigma, \Delta) = \frac{\sigma^2 + \Delta^2}{4G} - 2N_c \left\{ \tilde{\mathcal{M}} I_{\text{quad}} - \frac{1}{4} (\tilde{\mathcal{M}}^2 - 4\mu_I^2 \Delta^2) I_{\text{log}} + \int \frac{d^3 k}{(2\pi)^3} \left[\frac{\tilde{\mathcal{M}}^2 - 4\mu_I^2 \Delta^2}{4E_{k,0}^3} - \frac{\tilde{\mathcal{M}}}{E_{k,0}} - 2E_{k,0} + E_k^+ + E_k^- \right] \right\} \quad (2.28)$$

with the definitions $\tilde{\mathcal{M}} = \Delta^2 + M^2 - M_0^2$ and $E_{k,0} = \sqrt{k^2 + M_0^2}$. To obtain the expression for the isospin density we follow the same procedure used for the calculation of I_Δ and I_σ , but due to its different divergency structure we need to iterate the identity (2.18) once more. The final expression is

$$\langle n_I \rangle_{\text{NJL}}^{\text{MSS}} = 2\mu_I \Delta^2 I_{\text{log}} + 3\mu_I \left[\frac{\mathcal{M}^2}{4} + \mathcal{M}(M_0^2 - M^2) + M^2 \mu_I^2 + \frac{2\mu_I^2 M_0^2}{3} \right] I_1 + 2\mu_I I_2 - \frac{5\mu_I M^2}{4} [3\mathcal{M}^2 + 4\mu_I^2 M^2] I_4 + \frac{5\mu_I}{4} (4\mu_I^2 (M_0^2 - 2M^2) - 3\mathcal{M}^2) I_5 + I_6 \quad (2.29)$$

with the remaining definitions,

$$I_4 = \int \frac{d^3 k}{(2\pi)^3} \frac{1}{(k^2 + M_0^2)^{\frac{7}{2}}}, \quad (2.30)$$

$$I_5 = \int \frac{d^3 k}{(2\pi)^3} \frac{k^2}{(k^2 + M_0^2)^{\frac{7}{2}}}, \quad (2.31)$$

$$I_6 = \frac{35}{32} \sum_{j=\pm 1} \int \frac{d^3 k}{(2\pi)^3} \int_0^\infty \frac{t^3 dt}{\sqrt{1+t}} \times \frac{jE_k (\mathcal{M} - 2j\mu_I E_k)^4}{[(k^2 + M_0^2)t + (E_k + j\mu_I)^2 + \Delta^2]^{\frac{9}{2}}}. \quad (2.32)$$

Note that integrals I_1 to I_6 are all finite, and must be performed up to infinite in k . This is the fundamental difference between TRS, where we cut the whole integral in the cutoff Λ and MSS, where all finite medium contributions are separated and performed for the whole momentum range.

III. RESULTS

The parameter set used for the purpose of the present study are $m = 4.76$ MeV, $\Lambda = 659$ MeV and $G = 4.78$ GeV^{-2} which we have obtained by fitting the same value of the pion mass as used by Lattice QCD [62], i.e. $m_\pi = 131.7$ MeV, and other parameters as $f_\pi = 92.4$ MeV and $\langle \bar{\psi}\psi \rangle^{1/3} = -250$ MeV. This values corresponds to a vacuum mass $M_0 \simeq 303.5$ MeV.

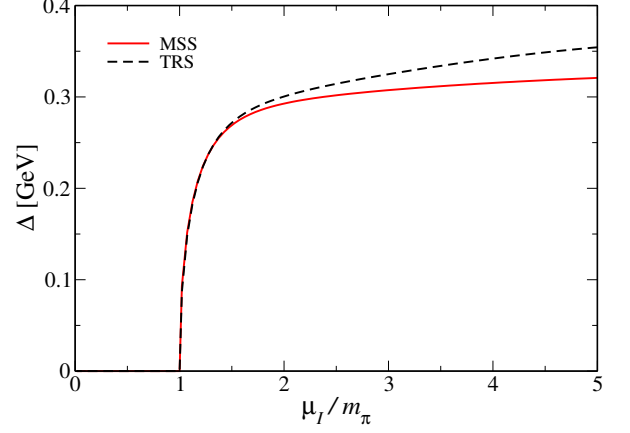


FIG. 1: Variation of the amplitude of the pion condensate Δ as a function of the normalized isospin chemical potential μ_I / m_π , using both TRS and MSS.

Figure 1 shows the variation of the pion condensate Δ with μ_I , scaled by the pion mass value. As might be seen from the plot, higher values of μ_I (starting from $\mu_I \sim 1.5m_\pi$) draw the differences between the two regularization processes. Notice that the values of Δ are increasingly larger for TRS than MSS when μ_I grows. At $\mu_I \sim \Lambda$ (i.e. $\mu_I \sim 5m_\pi$) the difference between TRS and MSS goes up to 30–35 MeV. This difference in Δ at higher values of μ_I also justifies the use of the medium separation scheme, specially since we are working at the zero temperature limit.

In the following part of this section we shall discuss our results for different relevant thermodynamic quantities within the two-flavor NJL model, comparing each one with the corresponding recent Lattice QCD results [46] and Chiral perturbation theory [54] results for both Leading Order (LO) and Next to Leading Order (NLO)¹.

In figures 2, 3 and 4, respectively, the variations of normalized pressure, isospin density and energy density are shown with respect to the isospin chemical potential scaled by m_π . These plots have mainly focussed on the region where $m_\pi \lesssim \mu_I \leq 2m_\pi$ as the region of interest,

¹ It is important to mention here that the preprint of Ref [54] is on the process of modification and in the present study we have used that modified datasets, collected through private communications [63].

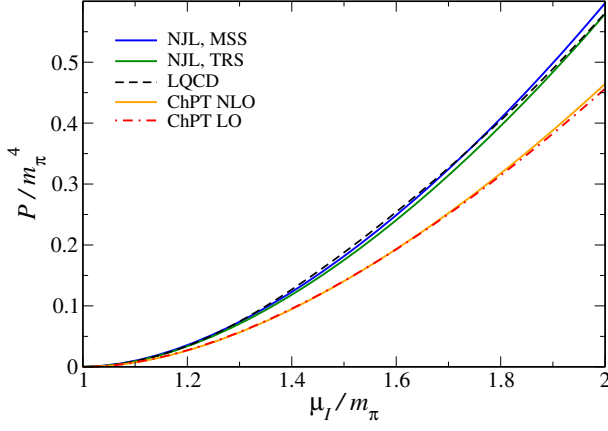


FIG. 2: Variation of the normalized pressure (P/m_π^4) as a function of the normalized isospin chemical potential μ_I/m_π . The behavior of MSS and TRS within the NJL model have been compared with LQCD results [46] and up to NLO results within χ PT [63]. The plot is specifically zoomed into the region of interest, up to the value of μ_I for which LQCD data is available.

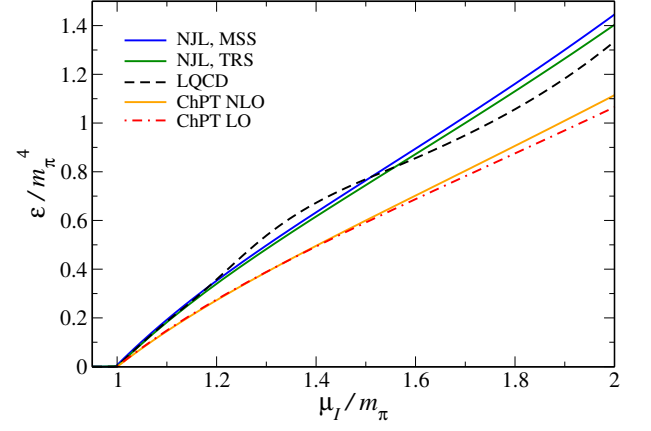


FIG. 4: Variation of the normalized energy density (ϵ/m_π^4) as a function of the normalized isospin chemical potential μ_I/m_π . The behavior of MSS and TRS within the NJL model have been compared with LQCD results [46] and up to NLO results within χ PT [63]. The plot is specifically zoomed into the region of interest, up to the value of μ_I for which LQCD data is available.

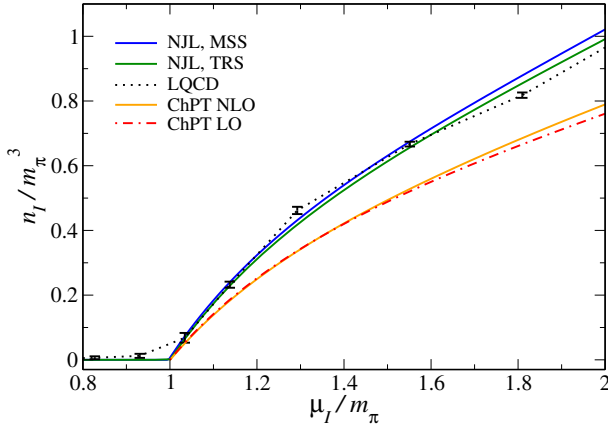


FIG. 3: Variation of the normalized isospin density (n_I/m_π^3) as a function of the normalized isospin chemical potential μ_I/m_π . The behavior of MSS and TRS within the NJL model have been compared with LQCD results [46] and up to NLO results within χ PT [63]. The plot is specifically zoomed into the region of interest, up to the value of μ_I for which LQCD data is available. Unlike the other thermodynamic quantities, here relatively fewer amount of lattice data points are shown with respective error bars. The dotted line represents the first order interpolation of the latter.

throughout which lattice QCD data was available². In this range of μ_I , the difference in results for TRS and MSS is relatively small, as evident from the plots. LO

and NLO results within χ PT have also been compared among others. Figure 2 distinctively shows the comparability between the NJL and LQCD results, specially in comparison with χ PT results up to NLO. Figures 3 and 4 show a typical behavior of LQCD data, which cross over the NJL TRS and MSS results around $\mu_I \sim 1.5m_\pi$, though overall being largely in agreement. This cross over could be due to the current unavailability of larger number of lattice data for isospin density.

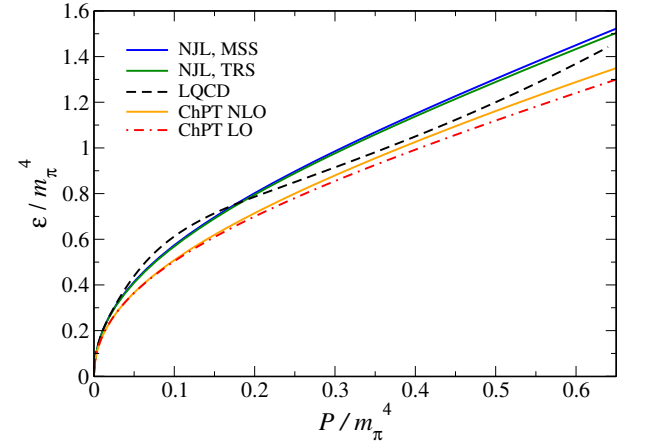


FIG. 5: Normalized equation of state. The behavior of MSS and TRS within the NJL model have been compared with LQCD results [46] and up to NLO results within χ PT [63]. The plot is specifically zoomed into the region of interest, up to the value of μ_I for which LQCD data is available.

² In general within Lattice QCD calculations, the maximum value of μ_I is constrained by the value of the lattice spacing.

Normalized EoS is presented in figure 5 where we can notice the reflection of the behavior of figures 3 and 4

regarding the comparability of NJL and LQCD results. Surprisingly, NLO χ PT results are in better agreement with the LQCD results for the region $0.3m_\pi^4 < P < 0.55m_\pi^4$, whereas NJL (TRS and MSS) results are in better agreement in the remaining region.

Finally in figure 6 we consider the full spectrum of μ_I , i.e. $0 \leq \mu_I \leq \Lambda$, particularly to emphasize the effect of the medium separation at higher values of μ_I on the normalized thermodynamic quantities P_{NJL} , $\langle n_I \rangle_{\text{NJL}}$ and ε_{NJL} as well as the EoS.

IV. CONCLUSIONS

In conclusion, we would like to emphasize on the fact that both the TRS and the MSS regularization schemes within the NJL model show promising results in the front of thermodynamic quantities describing systems similar to pion stars, being largely in agreement with the LQCD results. Regions with higher values of μ_I , where LQCD results are not available, we have predicted the pressure, isospin density, energy density and EoS both within TRS and MSS, highlighting the fact that MSS is more reliable in those regions due to its unique way of separating vacuum divergent effects from medium terms. In comparison with other effective theory results, i.e. χ PT, our results within the mean field NJL model show a better agreement with LQCD results which prompts us to further investigate the phase diagram for the region with finite μ_B and μ_I which is inaccessible by LQCD due to the sign problem. Also as mentioned in section I, the possibility of pion condensation in light of early universe dictates further exploration in the $T - \mu_I$ plane of the QCD phase diagram. Work in this direction is in progress.

V. ACKNOWLEDGEMENTS

This work was partially supported by Conselho Nacional de Desenvolvimento Científico e Tecnológico (CNPq) under grants 304758/2017-5 (R.L.S.F) and 6484/2016-1 (S.S.A) and as a part of the project INCT-FNA (Instituto Nacional de Ciência e Tecnologia - Física Nuclear e Aplicações) 464898/2014-5 (SSA), Coordenação de Aperfeiçoamento de Pessoal de Nível Superior (CAPES) (A.B) and Fundação de Amparo à Pesquisa do Estado de São Paulo (FAPESP) under Grant No. 2017/26111-4 (D.C.D).

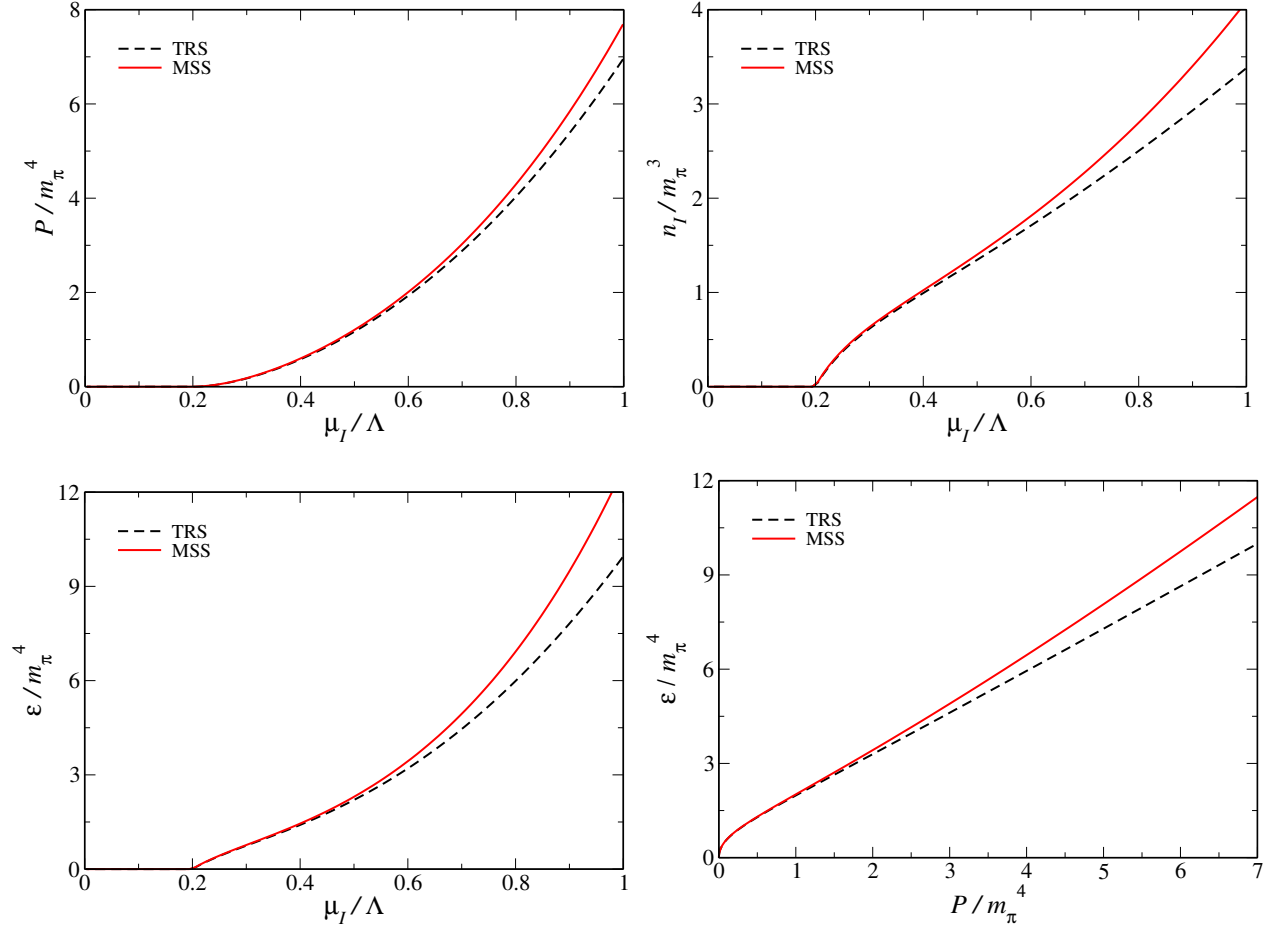


FIG. 6: Variations of normalized pressure (upper left panel), isospin density (upper right panel), and energy density (lower left panel) are shown as a function of isospin chemical potential scaled with the 3D momentum cutoff (μ_I/Λ) along with the normalized EoS (lower right panel). This plot shows the different behavior of MSS and TRS over the full spectrum of μ_I up to Λ .

-
- [1] K. Fukushima and T. Hatsuda, Rept. Prog. Phys. **74**, 014001 (2011) doi:10.1088/0034-4885/74/1/014001
- [2] M. G. Alford, A. Schmitt, K. Rajagopal and T. Schfer, Rev. Mod. Phys. **80**, 1455 (2008) doi:10.1103/RevModPhys.80.1455
- [3] F. Karsch, Lect. Notes Phys. **583**, 209 (2002) doi:10.1007/3-540-45792-56
- [4] S. Muroya, A. Nakamura, C. Nonaka and T. Takaishi, Prog. Theor. Phys. **110**, 615 (2003) doi:10.1143/PTP.110.615
- [5] P. F. Bedaque, EPJ Web Conf. **175**, 01020 (2018) doi:10.1051/epjconf/201817501020
- [6] J. B. Kogut and D. K. Sinclair, Phys. Rev. D **66**, 034505 (2002) doi:10.1103/PhysRevD.66.034505
- [7] J. B. Kogut and D. K. Sinclair, Phys. Rev. D **66**, 014508 (2002) doi:10.1103/PhysRevD.66.014508
- [8] D. T. Son and M. A. Stephanov, Phys. Rev. Lett. **86**, 592 (2001) doi:10.1103/PhysRevLett.86.592 [hep-ph/0005225].
- [9] D. T. Son and M. A. Stephanov, Phys. Atom. Nucl. **64**, 834 (2001) [Yad. Fiz. **64**, 899 (2001)] doi:10.1134/1.1378872
- [10] L. Lepori and M. Mannarelli, Phys. Rev. D **99**, no. 9, 096011 (2019) doi:10.1103/PhysRevD.99.096011
- [11] S. Carignano, L. Lepori, A. Mammarella, M. Mannarelli and G. Pagliaroli, Eur. Phys. J. A **53**, no. 2, 35 (2017) doi:10.1140/epja/i2017-12221-x
- [12] O. Janssen, M. Kieburg, K. Splittorff, J. J. M. Verbaarschot and S. Zafeiropoulos, Phys. Rev. D **93**, no. 9, 094502 (2016) doi:10.1103/PhysRevD.93.094502
- [13] T. D. Cohen and S. Sen, Nucl. Phys. A **942**, 39 (2015) doi:10.1016/j.nuclphysa.2015.07.018
- [14] E. S. Fraga, L. F. Palhares and C. Villavicencio, Phys. Rev. D **79**, 014021 (2009) doi:10.1103/PhysRevD.79.014021
- [15] M. Loewe and C. Villavicencio, Phys. Rev. D **67**, 074034 (2003) doi:10.1103/PhysRevD.67.074034
- [16] M. Loewe and C. Villavicencio, Phys. Rev. D **71**, 094001 (2005) doi:10.1103/PhysRevD.71.094001 [hep-ph/0501261].
- [17] K. Splittorff, D. T. Son and M. A. Stephanov, Phys. Rev. D **64**, 016003 (2001) doi:10.1103/PhysRevD.64.016003
- [18] J. O. Andersen, N. Haque, M. G. Mustafa and M. Strickland, Phys. Rev. D **93**, no. 5, 054045 (2016) doi:10.1103/PhysRevD.93.054045 [arXiv:1511.04660 [hep-ph]].
- [19] D. Ebert, T. G. Khunjua and K. G. Klimenko, Phys. Rev. D **94**, no. 11, 116016 (2016) doi:10.1103/PhysRevD.94.116016 [arXiv:1608.07688 [hep-ph]].
- [20] T. G. Khunjua, K. G. Klimenko, R. N. Zhokhov and V. C. Zhukovsky, Phys. Rev. D **95**, no. 10, 105010 (2017) doi:10.1103/PhysRevD.95.105010 [arXiv:1704.01477 [hep-ph]].
- [21] T. G. Khunjua, K. G. Klimenko and R. N. Zhokhov, Phys. Rev. D **98**, no. 5, 054030 (2018) doi:10.1103/PhysRevD.98.054030 [arXiv:1804.01014 [hep-ph]].
- [22] T. G. Khunjua, K. G. Klimenko and R. N. Zhokhov, Eur. Phys. J. C **79**, no. 2, 151 (2019) doi:10.1140/epjc/s10052-019-6654-2 [arXiv:1812.00772 [hep-ph]].
- [23] T. Xia, L. He and P. Zhuang, Phys. Rev. D **88**, no. 5, 056013 (2013) doi:10.1103/PhysRevD.88.056013
- [24] C. f. Mu, L. y. He and Y. x. Liu, Phys. Rev. D **82**, 056006 (2010). doi:10.1103/PhysRevD.82.056006
- [25] H. Abuki, R. Anglani, R. Gatto, M. Pellicoro and M. Ruggieri, Phys. Rev. D **79**, 034032 (2009) doi:10.1103/PhysRevD.79.034032
- [26] J. O. Andersen and L. Kyllingstad, J. Phys. G **37**, 015003 (2009) doi:10.1088/0954-3899/37/1/015003
- [27] G. f. Sun, L. He and P. Zhuang, Phys. Rev. D **75**, 096004 (2007) doi:10.1103/PhysRevD.75.096004
- [28] D. Ebert and K. G. Klimenko, Eur. Phys. J. C **46**, 771 (2006) doi:10.1140/epjc/s2006-02527-5
- [29] D. Ebert and K. G. Klimenko, J. Phys. G **32**, 599 (2006) doi:10.1088/0954-3899/32/5/001
- [30] L. He, M. Jin and P. Zhuang, Phys. Rev. D **74**, 036005 (2006) doi:10.1103/PhysRevD.74.036005
- [31] L. y. He, M. Jin and P. f. Zhuang, Phys. Rev. D **71**, 116001 (2005) doi:10.1103/PhysRevD.71.116001
- [32] L. He and P. Zhuang, Phys. Lett. B **615**, 93 (2005) doi:10.1016/j.physletb.2005.03.066
- [33] A. Barducci, R. Casalbuoni, G. Pettini and L. Ravagli, Phys. Rev. D **69**, 096004 (2004) doi:10.1103/PhysRevD.69.096004
- [34] D. Toublan and J. B. Kogut, Phys. Lett. B **564**, 212 (2003) doi:10.1016/S0370-2693(03)00701-9
- [35] M. Frank, M. Buballa and M. Oertel, Phys. Lett. B **562**, 221 (2003) doi:10.1016/S0370-2693(03)00607-5
- [36] S. Mukherjee, M. G. Mustafa and R. Ray, Phys. Rev. D **75**, 094015 (2007) doi:10.1103/PhysRevD.75.094015 [hep-ph/0609249].
- [37] A. Bhattacharyya, S. K. Ghosh, A. Lahiri, S. Majumder, S. Raha and R. Ray, Phys. Rev. C **89**, no. 6, 064905 (2014) doi:10.1103/PhysRevC.89.064905 [arXiv:1212.6134 [hep-ph]].
- [38] P. Adhikari, J. O. Andersen and P. Kneschke, Phys. Rev. D **98**, no. 7, 074016 (2018) doi:10.1103/PhysRevD.98.074016
- [39] R. Stiele, E. S. Fraga and J. Schaffner-Bielich, Phys. Lett. B **729**, 72 (2014) doi:10.1016/j.physletb.2013.12.053
- [40] H. Ueda, T. Z. Nakano, A. Ohnishi, M. Ruggieri and K. Sumiyoshi, Phys. Rev. D **88**, no. 7, 074006 (2013) doi:10.1103/PhysRevD.88.074006
- [41] K. Kamikado, N. Strodthoff, L. von Smekal and J. Wambach, Phys. Lett. B **718**, 1044 (2013) doi:10.1016/j.physletb.2012.11.055
- [42] B. B. Brandt, G. Endrödi and S. Schmalzbauer, Phys. Rev. D **97**, no. 5, 054514 (2018) doi:10.1103/PhysRevD.97.054514
- [43] B. B. Brandt, G. Endrödi and S. Schmalzbauer, EPJ Web Conf. **175**, 07020 (2018) doi:10.1051/epjconf/201817507020
- [44] B. B. Brandt and G. Endrödi, PoS LATTICE **2016**, 039 (2016) doi:10.22323/1.256.0039
- [45] B. B. Brandt, G. Endrödi and S. Schmalzbauer, arXiv:1811.06004 [hep-lat].
- [46] B. B. Brandt, G. Endrödi, E. S. Fraga, M. Hippert, J. Schaffner-Bielich and S. Schmalzbauer, Phys. Rev. D **98**, no. 9, 094510 (2018) doi:10.1103/PhysRevD.98.094510
- [47] J. A. Wheeler, Phys. Rev. **97**, 511 (1955).

- doi:10.1103/PhysRev.97.511
- [48] D. J. Kaup, Phys. Rev. **172**, 1331 (1968). doi:10.1103/PhysRev.172.1331
 - [49] P. Jetzer, Phys. Rept. **220**, 163 (1992). doi:10.1016/0370-1573(92)90123-H
 - [50] M. Colpi, S. L. Shapiro and I. Wasserman, Phys. Rev. Lett. **57**, 2485 (1986). doi:10.1103/PhysRevLett.57.2485
 - [51] S. L. Liebling and C. Palenzuela, Living Rev. Rel. **15**, 6 (2012) [Living Rev. Rel. **20**, no. 1, 5 (2017)] doi:10.12942/lrr-2012-6, 10.1007/s41114-017-0007-y
 - [52] H. Abuki, T. Brauner and H. J. Warringa, Eur. Phys. J. C **64**, 123 (2009) doi:10.1140/epjc/s10052-009-1121-0
 - [53] J. O. Andersen and P. Kneschke, arXiv:1807.08951 [hep-ph].
 - [54] P. Adhikari, J. O. Andersen and P. Kneschke, arXiv:1904.03887 [hep-ph].
 - [55] D. J. Schwarz and M. Stuke, JCAP **0911**, 025 (2009) Erratum: [JCAP **1010**, E01 (2010)] doi:10.1088/1475-7516/2009/11/025, 10.1088/1475-7516/2010/10/E01
 - [56] M. M. Wygas, I. M. Oldengott, D. Bdeker and D. J. Schwarz, Phys. Rev. Lett. **121**, no. 20, 201302 (2018) doi:10.1103/PhysRevLett.121.201302
 - [57] R. L. S. Farias, G. Dallabona, G. Krein and O. A. Battistel, Phys. Rev. C **73**, 018201 (2006) doi:10.1103/PhysRevC.73.018201
 - [58] V. V. Braguta and A. Y. Kotov, Phys. Rev. D **93**, no. 10, 105025 (2016) doi:10.1103/PhysRevD.93.105025
 - [59] R. L. S. Farias, D. C. Duarte, G. Krein and R. O. Ramos, Phys. Rev. D **94**, no. 7, 074011 (2016) doi:10.1103/PhysRevD.94.074011
 - [60] D. C. Duarte, R. L. S. Farias and R. O. Ramos, Phys. Rev. D **99**, no. 1, 016005 (2019) doi:10.1103/PhysRevD.99.016005
 - [61] S. P. Klevansky, Rev. Mod. Phys. **64**, 649 (1992). doi:10.1103/RevModPhys.64.649, T. Hatsuda and T. Kunihiro, Phys. Rept. **247**, 221 (1994) doi:10.1016/0370-1573(94)90022-1, M. Buballa, Phys. Rept. **407**, 205 (2005). doi:10.1016/j.physrep.2004.11.004
 - [62] B. B. Brandt and G. Endrödi, Private communications.
 - [63] P. Adhikari, J. O. Andersen, Private communications.